Comparison of Properties of Slow Pathway Potential between Successful and Unsuccessful Radiofrequency Applications in Patients who Underwent Catheter Ablation for Atrioventricular Nodal Reentrant Tachycardia

Hidekazu HIRAO, Yuji MURAOKA, Togo YAMAGATA,
Hideo MATSUURA and Goro KAJIYAMA

First Department of Internal Medicine, Hiroshima University School of Medicine, 1-2-3 Kasumi, Minami-ku, Hiroshima, 734-8551, Japan

ABSTRACT

Findings concerning selective slow pathway radiofrequency ablation for atrioventricular nodal reentrant tachycardia (AVNRT) using the slow pathway potential (SPP) guided method are reported. The electrogram at the SPP recording site showed double potentials consisting of the atrial potential (A) and SPP. However, SPP is usually recorded widely in the right atrial posteroseptal region. To examine whether there was any characteristic marker in the electrogram at the SPP recording site specific to successful RF application, the properties of SPP and its anatomical locations in both successful (S) (38 sites) and unsuccessful (UN) (28 sites) application sites were analyzed in 38 patients who underwent SPP-guided ablation. The distance between the upper margin of the coronary sinus ostium (UCSO) and the ablation catheter (ABL) ($D_{UCSO-ABL}$) was shorter in S than in UN (2.3 ± 6.3 mm vs. 9.0 ± 5.2 mm below the level of UCSO, p < 0.001). The interval between A and SPP (A-SPP) was longer in S than in UN (44.2 ± 9.9 msec vs. 24.0 ± 7.0 msec, p < 0.001). RF applications at the more anterior sites with longer A-SPP were more successful than at other sites. The sensitivity and specificity of A-SPP (more than 40 msec) were superior to those of $D_{UCSO-ABL}$ (within 5 mm) as the marker for the successful application (sensitivity; 73.7% v.s. 68.4%, specificity; 100% v.s. 82.1%, respectively). In conclusion, the sites with longer A-SPP might be specific for successful ablation.

Key words: Atrioventricular nodal reentrant tachycardia, Radiofrequency catheter ablation, Slow pathway potential, Upper margin of coronary sinus ostium

Atrioventricular nodal reentrant tachycardia (AVNRT) is one of the most common forms of supraventricular tachycardia. Dual atrioventricular nodal pathways in the perinodal tissue, being not only functionally but also anatomically distinct, are generally considered to be responsible for the pathogenesis of AVNRT. The permanent cure of AVNRT preserving atrioventricular (AV) nodal conduction was initially achieved by surgical ablation of the perinodal tissue[3,5,28,30]. The catheter ablation technique which can selectively ablate the fast[11,18,26] or slow[4,9,12,16,18,20,21,26,27,35,37–39] pathway has since been developed, and selective slow pathway ablation is now the dominantly used non-pharmacological curative therapy.

Selective radiofrequency (RF) catheter ablation of the slow pathway of the atrioventricular node is a well-established and highly effective treatment for AVNRT. Several studies have demonstrated a variety of approaches for the ablation of the slow pathways using anatomically[4,9,18,20,21,26,27,34,35,37–39] or electrically guided methods[12,16]. In anatomical approaches, the target site is determined primarily by means of anatomical fluoroscopic guidance. A relatively large number of RF applications are required for successful ablation and the possibility of the occurrence of AV block is relatively high. Several previous studies[8,13,18] have reported the limitations of an anatomically guided slow pathway ablative approach and the importance of electrically detailed mapping. In electrical approaches, either the "slow potential" as described by Haïssaguerre et al[12] or the "slow pathway potential (SPP)" as described by Jackman et al[16] are used to identify the ablation site. Jackman et al[16] reported that the sites of successful SPP-guided RF application were distributed broadly in the posteroseptal region between the coronary sinus ostium and the tricuspid annulus. Although the SPP recording sites are distributed over a wide

area in the posteroseptal region, not all RF applications at SPP recording sites successfully ablate the slow pathway. Recently, Yamane et al[39] reported that a successful ablation site was located around the level of the upper margin of the coronary sinus ostium. However, not all RF applications at sites around the level of the upper margin of the coronary sinus ostium could successfully ablate the slow pathway, and several RF applications at sites outside this area were often necessary in some of their patients. They did not clarify the electrical characteristics of SPP at the successful ablation sites. Although the efficacy of the SPP-guided approach in the slow pathway ablation of AVNRT has been described, the electrical characteristics in the potential specific to the effective RF energy application, the relationships between anatomical locations and local electrograms, and the anatomical origin of the double potentials consisting of SPP and atrial potential have not been sufficiently clarified. It is necessary to analyze the properties of the slow pathway potential and to determine more useful markers for successful ablation.

The purpose of this study was to characterize the properties of the electrogram at the SPP recording site and its anatomical location in both successful and unsuccessful RF applications in patients who finally underwent successful SPP-guided ablation.

MATERIALS AND METHODS

Patients. The study population consisted of 38 consecutive patients, 15 males and 23 females, with symptomatic AVNRT who underwent an electrophysiological study, in which SPP-guided RF catheter ablation was performed at Hiroshima University Hospital from April 1994 to April 1999. The mean age of the patients was 51.8 ± 15.8 years (range, 17–75 years). Thirty six patients had no organic heart disease. One patient had angina pectoris, and angiographs showed a 75% narrowing of the left anterior descending coronary artery. Another patient had pulmonary hypertension due to chronic pulmonary thromboembolism with deep vein thrombosis of the left common iliac vein. The indication for RF catheter ablation was either ineffective antiarrhythmic drug therapy, intolerant side effects of antiarrhythmic drugs, or unwillingness of the patient to undergo prophylactic, long-term drug therapy. The mean duration of symptoms was 11 ± 7.5 years (range, 1–31 years). A variety of antiarrhythmic drugs (mean, 1.7 ± 1.4, range, 1–6) were used for termination or prophylactic therapy against recurrent symptomatic tachyarrhythmias (Table 1). Written informed consent was obtained from all patients before the electrophysiological study and the ablation procedure.

Electrophysiological studies. Electrophysiological studies were performed using conventional methods with patients in a non-sedated, postabsorbed state. All antiarrhythmic medications had been discontinued for at least 72 hr before the study began. Under local anesthesia, three 6 or 2 Fr. quadripolar electrodes (Cordis-Webster Inc., Baldwin Park, CA, USA or Cardiac Pathways Corporation, Sunnyvale, CA, USA) were introduced through the femoral vein and located at the high right atrium, His-bundle region, and the right ventricular apex, respectively, under fluoroscopic guidance. A 7 Fr. decapolar coronary sinus electrode catheter with a lumen (Daig Inc. Minnetonka, MN, USA) was placed in the coronary sinus via the right subclavian vein. Heparin was administered as an intravenous bolus of 3,000 IU immediately after placement of the catheters, followed by an additional 1,000 IU every hour during the procedure. Intracardiac electrograms were recorded and stored digitally (1,000 samples/sec) on a Cardiolab system™ (Prucka Engineering Inc., Houston, TX, USA) simultaneously with surface electrocardiographs of leads I, II, III, V1, V5. Measurements were performed using the Cardiolab system at screen speeds of 200 mm/sec with on-screen digital calipers. Intracardiac electrograms were filtered at 30–500Hz. Programmed electrical stimulation was performed at the high right atrium using an eight-beat S1 drive at a cycle length of 600 and 500 msec with the introduction of single extra stimuli. The extra stimulus coupling interval was progressively decreased by 10 msec steps in each stimulating cycle until the atrial refractory period. The A_2H_2 duration recorded with each extra stimulus coupling interval was plotted against the A_1A_2 interval (measured in the His bundle electrogram) to construct an anterograde AV nodal function curve. An increase in the A_2H_2 interval of > 50 msec in response to a decrease in the A_1A_2 coupling interval of 10 msec was defined[19] as being anterograde dual physiology of the AV node. In the presence of the anterograde dual physiology of the AV node, the effective refractory period of the anterograde fast pathway was defined as being the longest A_1A_2 coupling interval that was conducted over the slow pathway. The anterograde effective refractory period of the slow pathway was defined as being the longest A_1A_2 interval that failed to propagate to the His-bundle. Rapid atrial pacing was achieved by increasing the atrial pacing rate from just faster than the sinus rate until AV Wenckebach conduction was observed. These programmed stimulation protocols were also performed to induce AVNRT. If AVNRT was not inducible at the baseline state, isoproterenol was infused at 1–2 μg/min, and atrial pacing procedures were repeated. Tachycardia was diagnosed as AVNRT by classic criteria[19] and by excluding intra-atrial reentrant tachycardia or tachycardia incorporating accessory pathways.

Radiofrequency catheter ablation. Radiofrequency catheter ablation was conducted immediately after the diagnostic electrophysiological study. A quadripolar electrode catheter with a 7 Fr. deflectable tip and a 4-mm long distal ablation electrode (2-mm interelectrode spacing) (EP Technologies Inc., Orchard Parkway, San Jose, CA, USA, or Osypca, Grenzach-Whylen, Germany, or Medtronic Inc., Minneapolis, MN, USA) was introduced into the right atrium via the femoral vein for mapping and ablation. While recording the electrogram from a distal pair of the mapping/ablation catheter, the area along the posteromedial tricuspid annulus between the His-bundle site and the coronary sinus ostium was carefully mapped during sinus rhythm. The SPP was defined as being a sharp and discrete deflection following the low amplitude and small atrial potentials that did not coincide with the His-bundle potential, as described by Jackman et al[16]. The atrial-to-ventricular electrogram ratio was also used as a guide with a value of < 0.5, suggesting that the catheter tip was located along the tricuspid ring[1,8,18,20,23,35,39]. RF current was delivered between the distal electrode of the ablation catheter and an adhesive skin patch placed on the patient's back, at 20 to 40 W using a unipolar fashion radiofrequency generator (EPT1000, HAT300, Atkar). Radiofrequency power, impedance, and tissue temperature were monitored continuously and were displayed during RF energy application. Power delivery was discontinued automatically when impedance exceeded 200 Ω. The occurrence of junctional rhythm during the application of RF energy has been considered as a useful marker for successful ablation[32]. RF energy was applied to the site where the slow pathway potential was clearly recorded during sinus rhythm for a total period of 60 to 90 sec when junctional rhythm occurred, unless an abrupt impedance rise was observed or the electrode was dislodged. If junctional rhythm during RF application did not occur, the application of RF energy was stopped for 30 sec. When the SPP was recorded widely along the mapped tricuspid annulus, RF application started at the most posteroinferior site, followed by anterior progression to the middle portion of the Koch's triangle which is bounded by the tendon of Todaro and the attachment of the septal leaflet of the tricuspid valve, with the coronary sinus ostium forming the base. During application of RF energy, AV conduction was carefully observed, and the energy was discontinued immediately when anterograde or retrograde conduction block developed. The inducibility of AVNRT was assessed after each application of the RF current. The endpoint for successful ablation was the elimination of slow pathway conduction, or the inability to induce AVNRT with or without one echo beat even during isoproterenol infusion at a rate of 1–2 μg/min.

Coronary sinus venography. Coronary sinus venography was performed by manual injection of contrast media using a 7 Fr. decapolar coronary sinus electrode catheter with a lumen (Daig Inc. Minnetonka, MN, USA). Venograms were obtained in two projections (50° left anterior oblique and 30° right anterior oblique views) and were stored on reel-to-reel cine tape for subsequent off-line analysis.

Data analysis. Data were obtained from 38 successful applications in all 38 patients and from 28 unsuccessful applications in 28 patients who required more than one application. For analysis of the unsuccessful applications, data for the first energy applications were used in the patients who required more than one application. The onset of SPP was defined as being the rise of the potential from the baseline between the atrial and ventricular electrograms.

1) **Properties of the slow pathway potential.** The interval between the atrial potential of the His-bundle electrogram and the atrial potential at the ablation site (HBEA-A), the interval between the atrial potential and SPP at the ablation site (A-SPP), the interval between SPP and the ventricular potential at the ablation site (SPP-V), the interval between the atrial potential at the ablation site and the atrial potential of the coronary sinus ostium (A-CSOA), the interval between the atrial potential of the coronary sinus ostium and SPP (CSOA-SPP), SPP duration, SPP amplitude, the ratio of the atrial potential amplitude to SPP amplitude at the ablation site (A / SPP), the ratio of SPP amplitude to the ventricular potential amplitude at the ablation site (SPP / V), and the ratio of the atrial potential amplitude to the ventricular potential amplitude at the ablation site (A / V) were analyzed (Fig. 1 A).

2) **Slow pathway potential recording site.** Using coronary sinus venography, the longitudinal vertical distance between the His-bundle electrogram catheter (HBE) and the lower margin of the coronary sinus ostium (LCSO) ($D_{HBE-LCSO}$), the longitudinal vertical distance between HBE and the ablation catheter tip (ABL) ($D_{HBE-ABL}$), and the longitudinal vertical distance between ABL and LCSO ($D_{ABL-LCSO}$) were measured at 30° to the right anterior oblique (RAO). The longitudinal vertical distance between the upper margin of the coronary sinus ostium (UCSO) and ABL ($D_{UCSO-ABL}$) and the longitudinal diameter of the coronary sinus ostium (D_{CSO}) were measured at 50° to the left anterior oblique (LAO) (Fig. 1 B). The ratio of $D_{ABL-LCSO}$ to $D_{HBE-LCSO}$ was calculated. All measurements were made at the ventricular end-systolic phase of the angiogram, using cinevideo edge detection methods (CAAS II / QUANTCOR, Pie Medica Imaging, Mastricht, Netherlands). The fluoroscopic image of the catheters was used to calibrate the
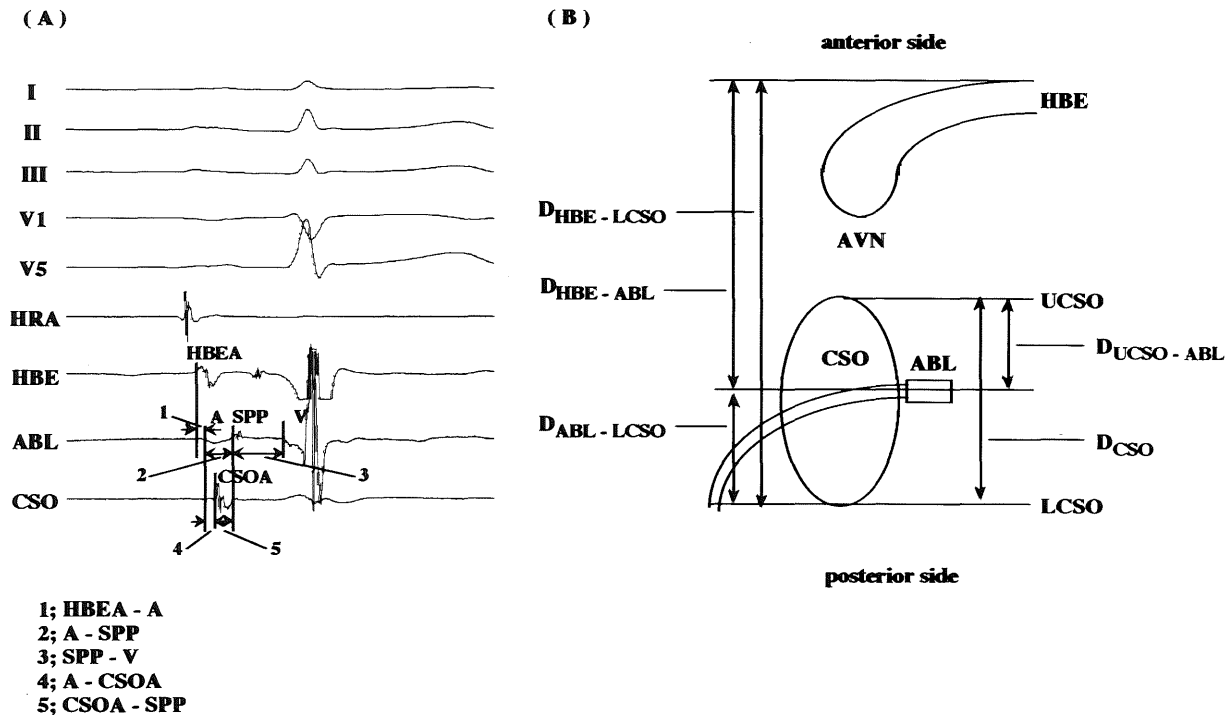
(A)   (B)

1; HBEA - A
2; A - SPP
3; SPP - V
4; A - CSOA
5; CSOA - SPP

Fig. 1. Definition of the measured electrogram parameters at ablation site with the slow pathway potential (**A**) and schematic representation of the measured anatomic distance in Koch's triangle (**B**).
A: HBEA, A, SPP, V, and CSOA indicate the atrial potential of the His-bundle electrogram, the atrial potential, the slow pathway potential, the ventricular potential at the ablation site, and the atrial potential of the coronary sinus ostium electrogram, respectively. HBEA-A (1), A-SPP (2), SPP-V (3), A-CSOA (4), and CSOA-SPP (5) indicate the interval between HBEA and A, the interval between A and SPP at the ablation site, the interval between SPP and V at the ablation site, the interval between A and CSOA, and the interval between CSOA and SPP, respectively. I, II, III, V1, V5 = surface electrocardiogram leads, HRA = high right atrial electrogram; HBE = His-bundle electrogram; ABL = ablation catheter electrogram; CSO = coronary sinus ostium electrogram. **B:** The longitudinal vertical distance between His-bundle electrogram catheter (HBE) and the lower margin of the coronary sinus ostium (LCSO) ($D_{HBE-LCSO}$), the longitudinal vertical distance between HBE and the ablation catheter tip (ABL) ($D_{HBE-ABL}$), the longitudinal vertical distance between ABL and LCSO ($D_{ABL-LCSO}$) were measured 30° to the right anterior oblique (RAO). The longitudinal vertical distance between the upper margin of the coronary sinus ostium (UCSO) and ABL ($D_{UCSO-ABL}$) and the longitudinal diameter of the coronary sinus ostium (D_{CSO}) was measured 50° to the left anterior oblique (LAO). AVN = atrioventricular node. CSO = coronary sinus.

size. Using the above parameters, the correlation between the properties of the electrogram at the ablation site and the location of the ablation catheter was analyzed.

Statistical analysis. All values are expressed as mean ± SD. Statistical analysis was performed by paired or unpaired Student's t-test. Correlation between the properties of the electrogram at the ablation site and the location of the ablation catheter was evaluated by linear regression analysis. A p value of < 0.05 was considered significant.

RESULTS

Results of ablation procedure. A common type of AVNRT was induced in all 38 patients. An uncommon type of AVNRT was also inducible in four patients. The mean cycle length of the tachycardia was 349.5 ± 58.2 msec. All patients in this study were successfully treated by RF application. The mean number of RF applications required was 3.4 ± 2.8 (range, 1–12, median, 2). Of the 38 slow

pathways, 10 were successfully ablated with a single energy application, while the other 28 required multiple applications. The mean power, temperature, and duration of each RF energy application were 32.6 ± 9.6 W (range, 20–45 W), 59.3 ± 7.2 °C (range, 48–70°C), and 61.4 ± 13.4 sec (range, 30–90 sec), respectively (Table 1). The electrophysiological effects of the finally successful ablation procedure in these 38 patients are described in Table 2. After successful slow pathway ablation, there was a significant increase in the AV node effective refractory period (before the first application, 261.9 ± 49.0 msec; after successful application, 292.3 ± 67.8 msec; p < 0.05) and a significant decrease in the fast pathway effective refractory period of the AV node (before the first application, 339.0 ± 85.2 msec; after successful application, 299.3 ± 66.0 msec; p < 0.05). There were no significant changes in the mean sinus cycle length (before the first application, 831.5 ± 156.1 msec; after successful application, 818.7 ± 142.8 msec; p

Table 1. Characteristics of the 38 Study Patients

Sex (Male/female)	15/23	
Age (year)	51.8 ± 15.8	(17 to 75)
Other heart disease		
None	36	
Ischemic heart disease	1	
Nonischemic heart disease	1	
Duration of symptoms (year)	11 ± 7.5	(1 to 31)
Prior antiarrhythmic drug trials	1.7 ± 1.4	(1 to 6)
Cycle length of AVNRT (msec)	349.5 ± 58.2	(240 to 470)
Number of RF applications	3.4 ± 2.8	(1 to 12)
Success with 1st RF application	10	
Mean Power of all applications (W)	32.6 ± 9.6	(20 to 45)
Mean Duration of all applications (sec)	61.4 ± 13.4	(30 to 90)
D $_{HBE-LCSO}$ (mm)	33.1 ± 7.0	(20.9 to 42.6)
D $_{CSO}$ (mm)	13.8 ± 3.7	(9.8 to 25.5)

Data are expressed as mean ± SD with ranges in parentheses. AVNRT = atrioventricular nodal reentrant tachycardia; RF = radiofrequency; D $_{HBE-LCSO}$ = distance between His-bundle electrogram catheter and the lower margin of the coronary sinus ostium; D $_{CSO}$ = longitidunal diameter of the coronary sinus ostium. D HBE-ABL = distance between His-bundle electrogram and the ablation catheter.

Table 2. Results and Electrophysiologic Effects of Slow Pathway Ablation

	Before the First Application	After Successful Application	p value
SCL (msec)	831.5 ± 156.1	818.7 ± 142.8	NS
AH interval (msec)	86.7 ± 17.1	82.4 ± 15.9	NS
HV interval (msec)	44.6 ± 7.0	45.0 ± 7.2	NS
AVN ERP (msec)	261.9 ± 49.0	292.3 ± 67.8	p<0.05
FP ERP (msec)	339.0 ± 85.2	299.3 ± 66.0	p<0.05
1:1 AVN conduction (/min)	146.5 ± 22	152.0 ± 28.6	NS
Dual physiology of AVN	32 (84.2%)	8 (21.0%)	p<0.001
Single AVN echo beat	38 (100%)	6 (15.8%)	p<0.001

Data are expressed as mean ± SD. SCL = sinus cycle length; AH interval = atrio-His interval; HV interval = His-ventricular interval; AVN ERP = effective refractory period of atrioventricular node; FP ERP = effective refractory period of the fast pathway; 1:1 AVN conduction = the maximal heart rate in which 1:1 atrioventricular conduction was maintained during high right atrium pacing; Dual physiology of AVN = an increase in the A_2H_2 interval of > 50 msec in response to a decrese in the A_1A_2 coupling interval of 10 msec of the atrial extrastimulus; Single AVN echo = one atrioventricular nodal reentrant atrial response.

= NS), the AH interval (before the first application, 86.7 ± 17.1 msec; after successful application, 82.4 ± 15.9 msec; p = NS), the HV interval (before the first application, 44.6 ± 7.0 msec; after successful application, 45.0 ± 7.2 msec; p = NS), and the fastest paced rate maintaining 1:1 anterograde AV conduction (before the first application, 146.5 ± 22.0 beats/min; after successful application, 152.0 ± 28.6 beats/min; p = NS). Dual physiology of AV node conduction was detected in 32 patients (84.2%) before the first RF application, and was detected in 8 patients (21.0%) after the final successful slow pathway ablation. Single AV node echo beats or AVNRT were induced in all 38 patients before the first RF application. Only single AV node echo beats were induced in 6 patients (15.8%) after the finally successful ablation. No patient had an inducible tachycardia or more than a single AV node echo beat after the successful slow pathway ablation. There were no complications such as AV conduction block in any of the patients.

Comparison of properties of the slow pathway potential and its recording site between successful and unsuccessful RF applications.
The characteristics of the slow pathway potential were compared between the 38 successful applications in all 38 patients and in the 28 unsuccessful applications in the 28 patients who required more than one application (Table 3, Fig. 2). For analysis of the characteristics of the unsuccessful applications, those of the first energy applications were used in the patients who required more than two applications. None of the SPP-V (80.4 ± 20.2 msec vs. 91.7 ± 25.9 msec), SPP duration (16.0 ± 5.4 msec vs. 16.0 ± 5.8 msec), SPP amplitude (0.12 ± 0.08 mV vs. 0.12 ± 0.10 mV), A / SPP (74.1 ± 50.4 % vs. 87.0 ± 79.6 %), SPP / V (21.3 ± 25.9 % vs. 15.1 ± 14.6 %), and A / V (10.8 ± 13.9 % vs. 11.9 ± 19.8 %) showed any significant difference between the successful and unsuccessful applications. HBEA-A in the successful applications was shorter than in the unsuccessful applications (28.6 ± 9.0 msec vs. 41.8 ± 13.9 msec, p < 0.001). A-SPP,

Table 3. Comparison of Properties of Slow Pathway Potential and its Recording Site in the Successful and Unsuccessful Radiofrequency (RF) Applications

	Successful Application	Unsuccessful Application	p value
HBEA-A (msec)	28.6 ± 9.0	41.8 ± 13.9	p<0.001
A-SPP (msec)	44.6 ± 9.1	24.0 ± 7.0	p<0.001
SPP-V (msec)	80.4 ± 20.2	91.7 ± 25.9	NS
A-CSOA (msec)	15.8 ± 10.0	4.3 ± 9.0	p<0.001
CSOA-SPP (msec)	28.7 ± 9.7	19.6 ± 7.7	p<0.001
SPP duration (msec)	16.0 ± 5.4	16.0 ± 5.8	NS
SPP amplitude (mV)	0.12 ± 0.08	0.12 ± 0.10	NS
A / SPP (%)	74.1 ± 50.4	87.0 ± 79.6	NS
SPP / V (%)	21.3 ± 25.9	15.1 ± 14.6	NS
A / V (%)	10.8 ± 13.9	11.9 ± 19.8	NS
D $_{UCSO\text{-}ABL}$ (mm)	−2.3 ± 6.3	−9.0 ± 5.2	p<0.001
D $_{ABL\text{-}LCSO}$ / D $_{HBE\text{-}LCSO}$ (%)	34.8 ± 17.3	14.3 ± 14.9	p<0.001
D $_{HBE\text{-}ABL}$ (mm)	21.0 ± 7.5	29.8 ± 8.7	p<0.001
Junctional rhythm during RF application (%)	94.7	21.4	p<0.001

Data are expressed as mean ± SD. HBEA-A = the interval between the atrial potential of His-bundle electrogram and the atrial potential at the ablation site; A-SPP = the interval between the atrial potential and the slow pathway potential at the ablation site; SPP-V = the interval between the slow pathway potential and the ventricular potential at the ablation site; A-CSOA = the interval between the atrial potential at the ablation site and the atrial potential of coronary sinus ostium; CSOA-SPP = the interval between the atrial potential of coronary sinus ostium and the slow pathway potential at the ablation site; SPP duration = duration of the slow pathway potential; SPP amplitude = amplitude of the slow pathway potential; A / SPP = the ratio of the amplitude of the atrial potential to the amplitude of the slow pathway potential; SPP / V = the ratio of the amplitude of the slow pathway potential to the ventricular potential; A / V = the ratio of the amplitude of the atrial potential to the amplitude of the ventricular potential; D UCSO-ABL = the distance between the upper margin of the coronary sinus ostium and the ablation catheter tip; D $_{ABL\text{-}LCSO}$ / D $_{HBE\text{-}LCSO}$ = the ratio of the distance between the ablation catheter tip and the lower margin of the coronary sinus ostium to the distance between the His-bundle electrigram catheter and the lower margin of the coronary sinus ostium; D $_{HBE\text{-}ABL}$ = distance between His-bundle electrogram catheter and the ablation catheter tip.

A-CSOA, and CSOA-SPP in the successful applications were longer than in the unsuccessful applications (44.2 ± 9.9 msec vs. 24.0 ± 7.0 msec, p < 0.001; 15.8 ± 10.0 msec vs. 4.3 ± 9.0 msec, p < 0.001; 28.7 ± 9.7 msec vs. 19.6 ± 7.7 msec, p < 0.001, respectively). The ratios of D$_{ABL\text{-}LCSO}$ to D$_{HBE\text{-}LCSO}$ in the successful applications were greater than in the unsuccessful applications (34.8 ± 17.3 % vs. 14.3 ± 14.9 %, p < 0.001). The D$_{UCSO\text{-}ABL}$ in the successful applications was shorter than in the unsuccessful applications (2.3 ± 6.3 mm vs. 9.0 ± 5.2 mm below the level of UCSO, p < 0.001). The D$_{HBE\text{-}ABL}$ in the successful applications was shorter than in the unsuccessful applications (21.0 ± 7.5 mm vs. 29.8 ± 8.7 mm, p < 0.001). The occurrence of junctional rhythm during RF application was more frequent in the successful applications than in the unsuccessful applications (94.7% vs. 21.4%, p < 0.001). Although HBEA-A, A-CSOA, and CSOA-SPP showed significant differences between the successful and the unsuccessful applications, there was a large variance in the data of each parameter. The ranges of these parameters measured in the successful application sites and in the unsuccessful application sites were not well demarcated (Fig. 2). It was difficult to determine the cut off value for the optimal RF application site. The ranges of A-SPP and the ablation catheter position (D$_{UCSO\text{-}ABL}$) measured in the successful application sites and in the unsuccessful application sites were relatively demarcated. A-SPP was more than 40 msec at 28 sites (73.7%) of the 38 successful application sites, and no more than 40 msec at any of the 28 unsuccessful application sites. The anatomical catheter locations were more anterior than the level of 5 mm below UCSO at 26 sites (68.4%) of the 38 successful application sites, and at 5 sites (17.9%) of the 28 unsuccessful application sites. All RF applications at sites where A-SPP was more than 40 msec were successful despite the anatomical catheter locations. On the contrary, RF applications at sites where A-SPP was less than 40 msec were unsuccessful even if the anatomical catheter locations were more anterior than the level of 5 mm below UCSO (Fig. 4). The sensitivity and specificity of the cut off value at which A-SPP was more than 40 msec were 73.7 % and 100%, respectively. The sensitivity and specificity of the cut off value at which the anatomical catheter locations were more anterior than the level of 5 mm below UCSO were 68.4 % and 82.1%, respectively. The A-SPP was more useful than the anatomical catheter location for successful ablation. As a whole, the sites at which A-SPP was more than 40 msec and the sites around UCSO might be specific for successful applications. Representative recordings of the slow pathway potential at each site are provided (Fig.
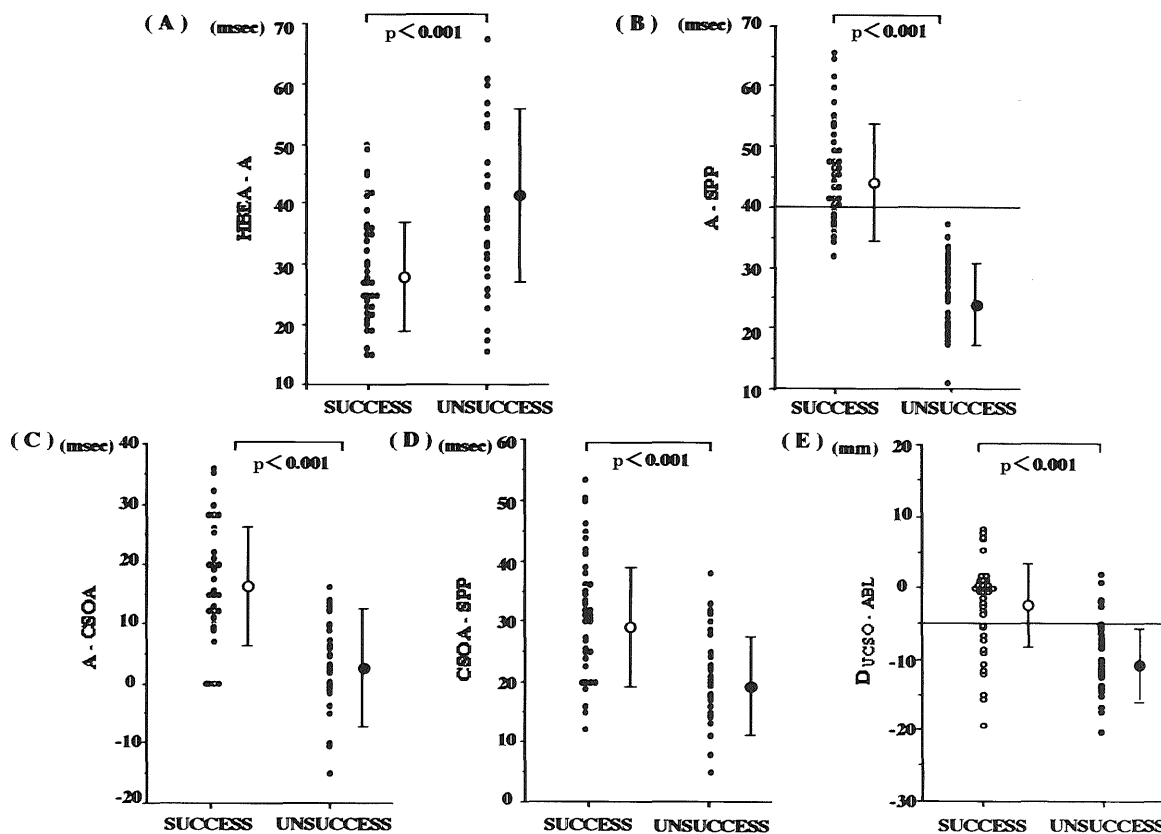
Fig. 2. Comparison of the properties of the slow pathway potential in the successful and unsuccessful application sites.
A: The interval between the atrial potential of the His-bundle electrogram and the atrial potential at the ablation site (HBEA-A) in the successful applications was shorter than in the unsuccessful applications. **B:** The interval between the atrial potential and the slow pathway potential at the ablation site (A-SPP); **C:** the interval between the atrial potential at the ablation site and the atrial potential of the coronary sinus ostium (A-CSOA), and **D:** the interval between the atrial potential of the coronary sinus ostium and the slow pathway potential at the ablation site (CSOA-SPP) in the successful applications were all longer than in the unsuccessful applications. **E:** The distance between the upper margin of the coronary sinus ostium and the ablation catheter tip (D$_{UCSO-ABL}$) in the successful applications was shorter than in the unsuccessful applications. It is notable that the most successful ablation sites were distributed around the level of UCSO.

3). It is noteworthy that HBEA-A in the successful application site was shorter, A-SPP, A-CSOA, and CSOA-SPP in the successful application site were longer than in the unsuccessful application site, and the ablation catheter tip in the successful application site was located more anteriorly compared to that in the unsuccessful application site, and was located around the upper margin of the coronary sinus ostium.

Dimension of Koch's triangle. The measured D$_{HBE-LCSO}$ and D$_{CSO}$ by coronary sinus venography were 33.1 ± 7.0 mm (range; 20.9 to 42.6 mm) and 13.8 ± 3.7 mm (range; 9.8 to 25.5 mm). There was a marked variability in D $_{HBE-LCSO}$ and D $_{CSO}$ (Table 1).

Properties of the slow pathway potential and its recording site. To characterize the successful application site, the relationships between D$_{UCSO-ABL}$ and the properties of SPP in both the successful and unsuccessful RF applications were evaluated in all patients. The D$_{UCSO-ABL}$ correlated significantly with HBEA-A, A-SPP, SPP-V, A-CSOA,

and CSOA-SPP, respectively (r =−0.50, p < 0.001; r = 0.54, p < 0.001, r =−0.32, p < 0.05; r = 0.35, p < 0.05; r = 0.37, p < 0.05, respectively) (Fig. 4). As the SPP recording site shifted more to the anterior position, HBEA-A and SPP-V became shorter, and A-SPP, A-CSOA, and CSOA-SPP became longer. In other words, as the SPP recording site shifted more to the anterior position, the timing of the appearance of the atrial potential became earlier and that of the SPP became later. The atrial potential and SPP showed a different activation sequence. There was no significant correlation between D$_{UCSO-ABL}$ and SPP duration or SPP amplitude. Also, there was no significant correlation between D$_{UCSO-ABL}$ and A / SPP, SPP / V, A / V. The SPP duration, SPP amplitude, and the amplitude of A, SPP, and V remained unchanged even though the SPP recording site shifted more to the anterior position.

DISCUSSION

This study was conducted to characterize the

(A) Successful RF application site

(B) Unsuccessfu RF application site

HBEA - A = 21 msec
A - SPP = 63 msec
SPP - V = 60 msec
A - CSOA = 25 msec
CSOA - SPP = 41 msec

HBEA - A = 60 msec
A - SPP = 18 msec
SPP - V = 72 msec
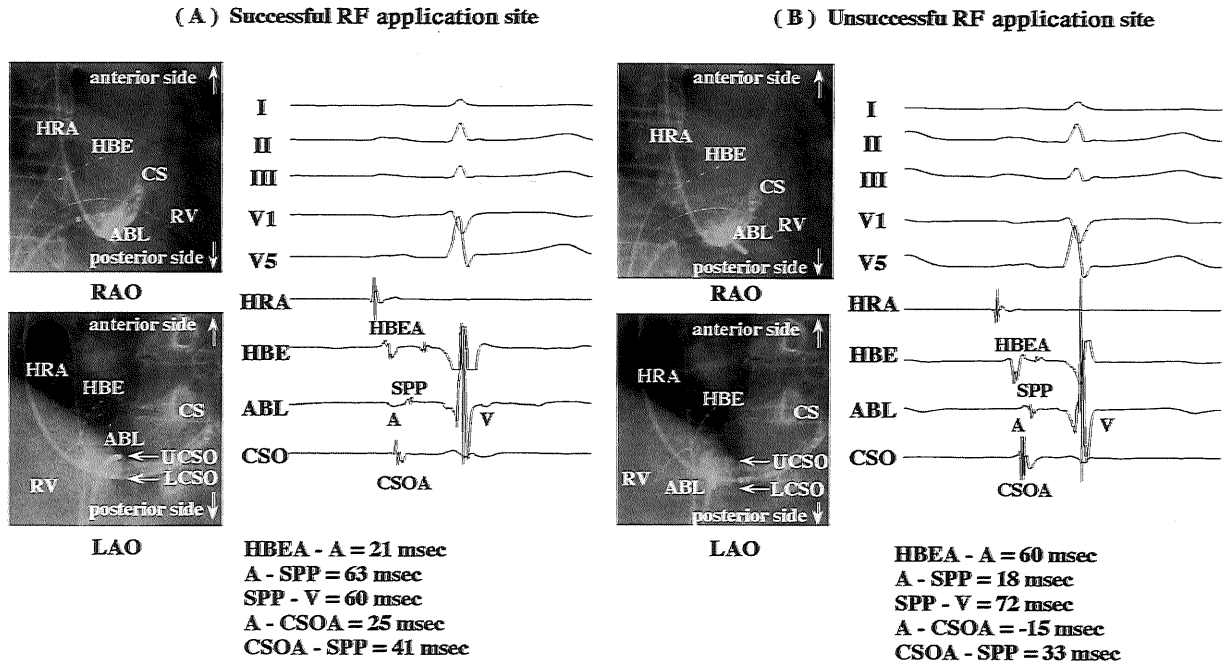A - CSOA = -15 msec
CSOA - SPP = 33 msec

Fig. 3. Recordings of the slow pathway potential and its recording site in the successful (A) and the unsuccessful (B) radiofrequency energy applications in patients with atrioventricular nodal tachycardia are shown.
 Note that the interval between the atrial potential (A) and the slow pathway potential (SPP) at the ablation site (A-SPP), the interval between A and the atrial potential of the coronary sinus ostium (CSOA) (A-CSOA), and the interval between CSOA and SPP (CSOA-SPP) were all longer, while the interval between the atrial potential of the His-bundle electrogram (HBEA) and A (HBEA-A) and the interval between SPP and the ventricular potential at the ablation site (V) (SPP-V) were shorter in the successful ablation site than in the unsuccessful ablation site. The ablation catheter tip in the successful ablation site was located more anteriorly compared to that in the unsuccessful ablation site and was located around the upper margin of the coronary sinus ostium. HRA = high right atrial catheter and electrogram; HBE = His-bundle electrogram catheter and electrogram; RV = right ventricular catheter; CS = coronary sinus catheter; ABL = ablation catheter and electrogram; CSO = coronary sinus ostium electrogram; UCSO = upper margin of the coronary sinus ostium; LCSO = lower margin of the coronary sinus ostium; I, II, III, V1, V5 = surface electrocardiogram leads.

properties of the electrogram at the SPP recording site and its anatomical location in successful SPP-guided RF applications and to evaluate the relationship between the former and latter parameters. The longer interval between the atrial potential and SPP might be specific for successful RF applications. Although the electrogram parameters correlated to the anatomical location at the SPP recording site, the A-SPP interval was a superior marker to the anatomical catheter location in successful applications. Especially, an A-SPP interval of more than 40 msec was a useful marker in successful applications. The most successful ablation sites were more anterior than the level of 5 mm below UCSO. However, RF applications at sites where A-SPP was less than 40 msec were unsuccessful even if the anatomical location of the ablation catheter was more anterior than the level of 5 mm below UCSO. All RF applications at sites where A-SPP was more than 40 msec were successful despite the anatomical catheter locations. As the SPP recording site shifted more to the anterior position, the timing of the appearance for the atrial potential became earlier, while

that for the SPP became later. The atrial potential and SPP showed a different activation sequence. The atrial potential and SPP may be caused by the asynchronous activation of the atrial septal wall and the slow pathway.

Characteristics of the slow pathway potential indicative of successful ablation.

Many studies have demonstrated a variety of approaches regarding the slow pathways. In the anatomical approach, the target site is determined primarily on anatomical guidance[4,9,18,20,21,26,27,35,37-39]. RF current applied at the region between the tricuspid annulus and the coronary sinus ostium refers only to fluoroscopic anatomical location. If one application is unsuccessful, a series of applications are repeated at progressively higher levels approaching the AV node. Thereafter, as Wu et al[37] reported, a direct midseptal approach as a simple technique is advised, in which RF application is achieved at the right atrial midseptum primarily based on anatomical fluoroscopic guidance. Although the success rate was high, a relatively large number of RF applications were required and the possibility of AV block was slightly high.
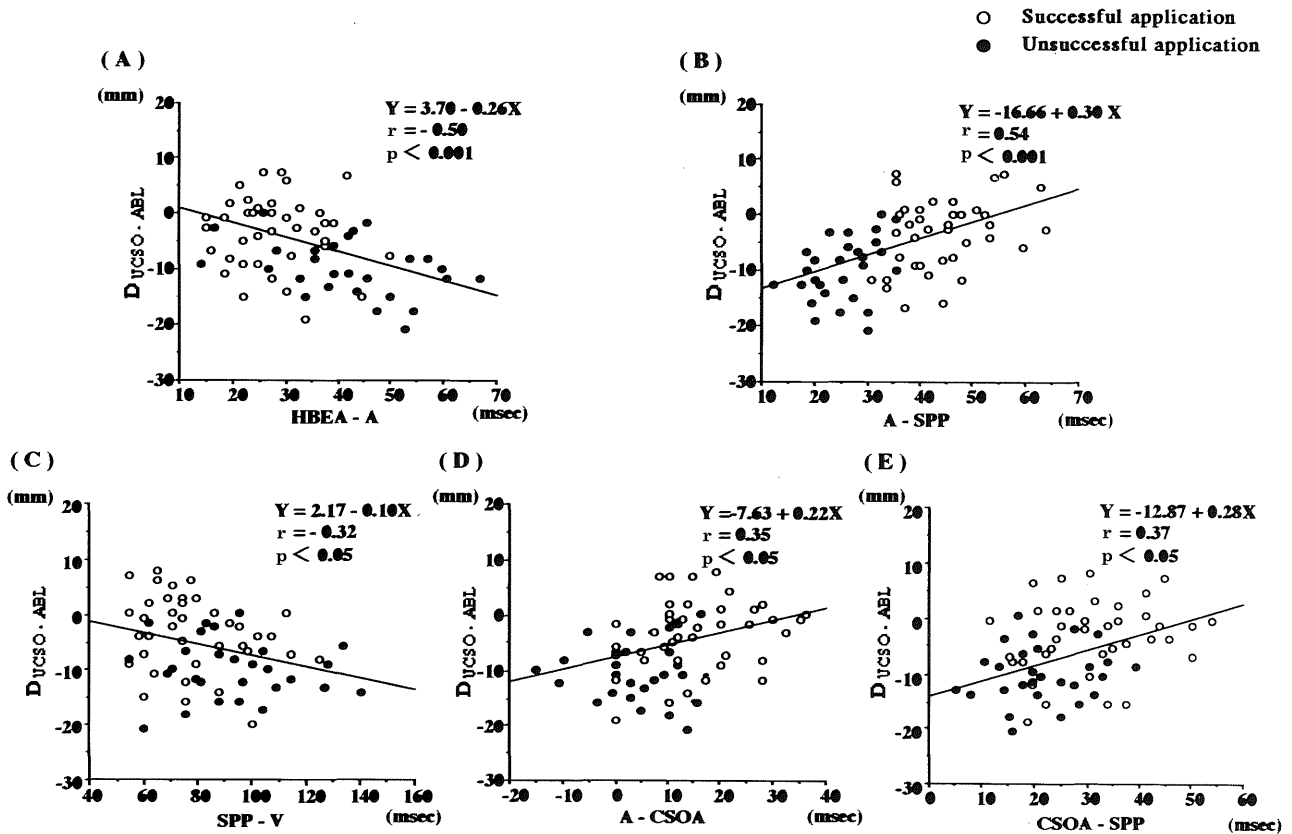
Fig. 4. Scatter plots showing **A:** the relation between the distance between the upper margin of the coronary sinus ostium (UCSO) and the ablation catheter tip (ABL) ($D_{UCSO-ABL}$), and the interval between the atrial potential of the His-bundle electrogram and the atrial potential at the ablation site (HBEA-A); **B:** the relation between $D_{UCSO-ABL}$ and the interval between the atrial potential and the slow pathway potential at the ablation site (A-SPP); **C:** the relation between $D_{UCSO-ABL}$ and the interval between the slow pathway potential and the ventricular potential at the ablation site (SPP-V); **D:** the relation between $D_{UCSO-ABL}$ and the interval between the atrial potential at the ablation site and the atrial potential of the coronary sinus ostium catheter (A-CSOA); **E:** the relation between $D_{UCSO-ABL}$ and the interval between the atrial potential of the coronary sinus ostium catheter and the slow pathway potential (CSOA-SPP). The $D_{UCSO-ABL}$ correlated significantly with HBEA-A, A-SPP, SPP-V, A-CSOA, and CSOA-SPP, respectively (r =−0.50, p < 0.001; r = 0.54, p < 0.001, r =−0.32, p < 0.05; r = 0.35, p < 0.05; r = 0.37, p < 0.05, respectively). As the slow pathway potential recording site shifted more to the anterior position, HBEA-A and SPP-V became shorter, and A-SPP, A-CSOA, and CSOA-SPP became longer. As the slow pathway potential recording site shifted more to the anterior position, the timing of the atrial potential became earlier and the timing of the slow pathway potential became later.

Recently, Ueng et al[34] reported that the site of successful ablation was about 13 mm from the His-bundle electrograms. In our study, the distance between the His-bundle electrogram catheter and the ablation catheter in successful applications was 21.0 ± 7.5 mm. Our results were not compatible with theirs. This discrepancy might be due to the different methodologies employed in the measurement of each landmark for the Koch's triangle or to the different patient populations. Yamane et al[39] also reported that the successful ablation site was located within 5 mm above and below the level of the upper margin of the coronary sinus. Their results were excellent in that the optimal target site was relatively confined to around the upper margin of the coronary sinus ostium. However, single RF application could successfully ablate the slow pathway in only 78% of their

patients. Not all RF applications at sites within 5 mm above and below the level of the upper margin of the coronary sinus could successfully ablate the slow pathway, and several RF applications at sites outside 5 mm above and below the level of the upper margin of the coronary sinus ostium were often necessary in the remaining 22% of their patients. The kind of landmark used for such patients was not mentioned. In our study, the anatomical catheter locations were more anterior than the level of 5 mm below UCSO in 68.4% of successful application sites. Our finding was compatible with their results. However, RF applications at sites where A-SPP was less than 40 msec were unsuccessful even if the anatomical catheter locations were more anterior than the level of 5 mm below UCSO. RF applications at sites where A-SPP interval was more than 40 msec were suc-

cessful despite the anatomical catheter locations. The sensitivity and specificity of the sites at which A-SPP were more than 40 msec were 73.7 % and 100%, respectively. The sensitivity and specificity of the sites at which the anatomical catheter locations were more anterior than the level of 5 mm below UCSO was 68.4 % and 82.1%, respectively. The A-SPP interval was a superior marker to the anatomical catheter location for the successful application. Our study suggests that the A-SPP interval provides a useful electrical marker in addition to the anatomical ablation catheter location for the optimal target site. Several previous studies[8,13,18] have reported limitations in the anatomically guided slow pathway ablative approach, and the importance of electrically detailed mapping. The anatomical ablation catheter position may not reflect exactly the full three-dimensional complexity of this area and there is a marked variability concerning the anatomy of Koch's triangle. The RF application according to the anatomical guidance might increase the risk of AV block, if the fast AV node pathways deviate posteriorly and are situated in the posteroseptal right atrium. In the electrical approach, the "SPP" described by Jackman et al[16] or the "slow potential" described by Haïssaguerre et al[12] is used to identify the target site. The slow potential was recorded as a low frequency deflection with high frequency atrial deflection and differed from SPP. The zone in which the slow potential was recorded was anterior to the SPP recording site described by Jackman et al[16]. Although slow pathway ablation using either potentials is a safe and effective treatment for AVNRT, we preferred to use the slow pathway potential that was recorded farther away from the His-bundle, primarily to avoid complications such as AV conduction block. Although many studies have reported that the application of the RF energy guided by the SPP is safe and effective, the electrical characteristics of SPP as specific markers for successful ablation remain undetermined. In the present study, we used the SPP as a marker for slow pathway ablation. HBEA-A in the successful applications was shorter than in the unsuccessful applications. A-CSOA, and CSOA-SPP in the successful applications were all longer than in the unsuccessful applications. Although these parameters showed significant differences between the successful and unsuccessful applications, there was a large variance in the data of each parameter. The ranges of each parameter measured in the successful and unsuccessful application sites were not well demarcated. It was difficult to determine the cut off value for the optimal RF application site. The ranges of A-SPP measured in the successful and unsuccessful application sites were relatively demarcated. A-SPP were relatively specific to the successful

applications. Although parameters other than A-SPP also correlated statistically with the anatomical location, none of the correlations was so strong. The electrical parameters may not reflect exactly the anatomical location.

Supposed substrate for the successful slow pathway ablation site and the origin of the atrial potential and the slow pathway potential. The anatomical substrate for the successful ablation site guided by SPP remains to be determined. The local electrogram consisting of the atrial potential and SPP shows the double potentials. In the present study, as the ablation catheter shifted more to the anterior position, the timing of the appearance for the atrial potential became earlier and that for SPP became later. The atrial potential and SPP showed different activation sequences. In isolated, blood-perfused porcine and canine hearts[22,23], it has been suggested that low frequency deflections followed by high frequency deflections may be caused by asynchronous activation of two muscle bands above and below the coronary sinus ostium, and that low frequency deflection may be caused by a far-field signal and high frequency deflection by local activation of transitional cells in the region between the coronary sinus ostium and the tricuspid annulus. In other previous mapping studies[6,7,22], the electrical wavefront during sinus rhythm approached Koch's triangle from the anterior side then swept posteriorly and then its direction was changed to pass anteriorly toward the AV node via the slow pathway. From such evidence, our findings indicated that the sequence of the atrial potential might reflect atrial activation from the anterior to posterior direction close to the ablation catheter, and that the slow pathway potential might reflect the local activation from the posterior to anterior direction at the right atrial posteroseptum between the coronary sinus ostium and the tricuspid annulus (Fig. 5).

Histological and electrophysiological descriptions of the AV node have shown the posterior extension of the AV node running parallel to the tricuspid annulus[1,15,24,29,33]. The cellular architecture[1,15,17,33] and electrophysiological properties of the posterior extensions[2,29,36] change gradually from atrial cells to AV nodal cells as the location in the posterior extension reaches the anterior side. Inoue and Becker[15] demonstrated the presence of a rightward extension in autopsied hearts. This extension could be traced to underneath the anterior margin of the coronary sinus ostium. These fibers could account for conduction over the slow AV nodal pathway. In our study and the study of Yamane et al, the RF applications at sites around UCSO were effective in most of the patients. This finding led us to speculate that the substrate of the successful site might include the extended compact AV node reaching to the upper
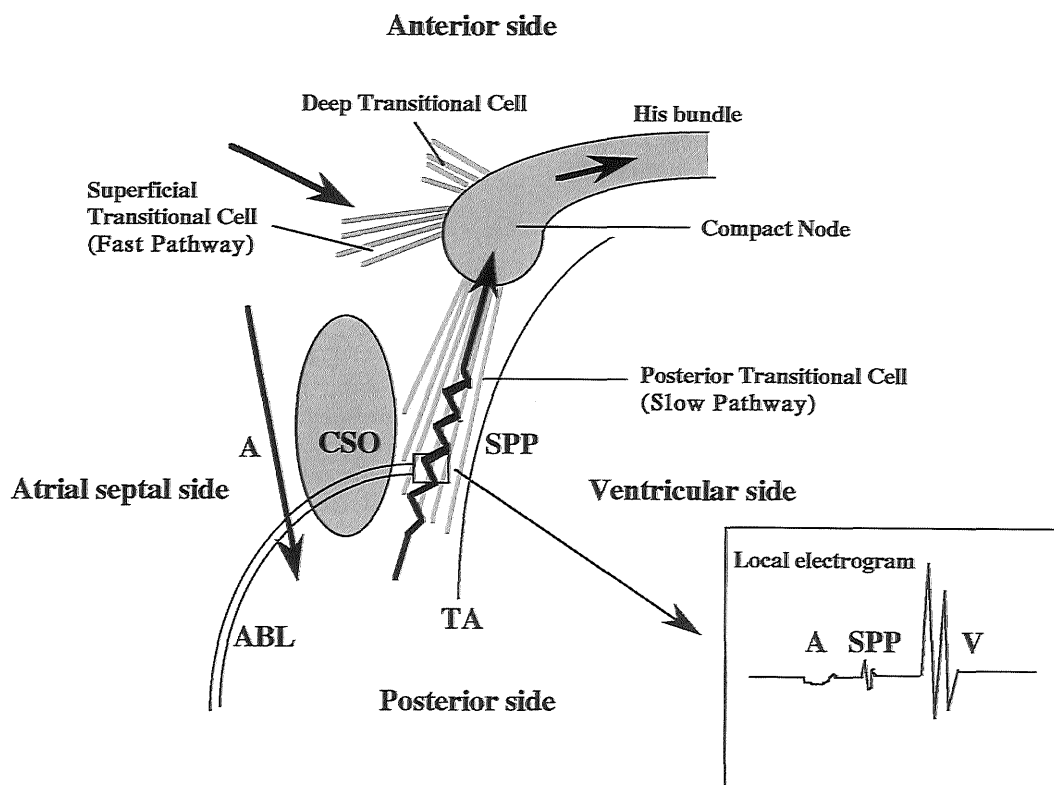
Fig. 5. Hypothetical schema of the anatomy of the atrioventricular node and the excitation sequence within Koch's triangle.
The atrioventricular node consists of the compact node and the transitional cells. The excitation from the atrium approaches the compact node via the transitional cells. The inputs to the compact node were divided into the fast pathway and the slow pathway. The fast pathway consisted of the deep transitional cells and the superficial transitional cells. The slow pathway consisting of the posterior transitional cells, runs along the posteroseptal region between the coronary sinus ostium (CSO) and the tricuspid valve annulus (TA). The atrial electrical activation (A) approached Koch's triangle, then swept posteriorly so that the apex of the triangle was activated before its base, and then its direction was changed to pass anteriorly toward the atrioventricular node in the region that records the slow pathway potential (SPP) during sinus rhythm. There were multiple and different posterior inputs to the atrioventricular node in the posteroseptal region. The local electrogram from the ablation catheter tip (ABL) consisted of A, SPP and the ventricular electrogram (V).

margin of the coronary sinus ostium.

In other previous reports[3,10,24,31], multiple and electrophysiologically different posterior inputs in the posteroseptal region have been suggested. In the present study, SPP was recorded over a wide area in the posteroseptal region. Theoretically, successful RF application may be achieved by the interruption of the posterior extension at various points along its length. In clinical ablation cession, all RF applications at the sites where SPP was recorded were not always successful. These findings suggested that all slow pathways may not necessarily be related to the formation of AVNRT. It is important to ablate the critical slow pathway which is essential for the formation of AVNRT. In our study, among the sites where SPP was recorded in the posteroseptal region, the RF applications at sites with longer A-SPP were more effective than at the other sites. The longer A-SPP interval may indicate that the SPP recording sites contain a slow pathway with a slower conduction property. These findings may explain why not all RF appli-

cations at sites around the level of the upper margin of the coronary sinus could successfully ablate the slow pathway and why RF applications at sites with a longer A-SPP interval were more effective.

Study Limitations. This study had several limitations. First, identification of possible SPP was based solely on electrically morphological criteria of SPP, and no pacing maneuver was performed to observe the relationship between the conduction property and potential morphology. In a previous study[16], other electrophysiological characteristics of SPP were demonstrated, namely, that the order of the atrial potential and SPP was reversed during retrograde slow pathway conduction, and an atrial extra stimulus during AVNRT did not reset the SPP despite the resetting of atrial activation. Second, the initial energy application site was not randomized. The initial energy application was delivered at the most posteroinferior site where SPP was recorded in each patient to avoid AV conduction block. Thus, the effect of

energy application to the anterior portion of the area with the SPP recording could not be fully evaluated. However, all patients in this study were successfully treated only at the posterior portion with the SPP recording by RF applications. Third, the two-dimensional measurements of Koch's triangle, based on catheter positions in this study, may not accurately represent the true distances of the three-dimensional structures of Koch's triangle.

ACKNOWLEDGMENTS

REFERENCES

1. Anderson, R.H., Becker, A.E., Brechenmacher, C., Davies, M.J. and Rossi, L. 1975. The human atrioventricular junctional area: a morphological study of the A-Vnode and bundle. Eur. J. Cardiol. **3**: 11–25.
2. Anderson, R.H., Janse, M.J., van Capelle, F.J., Billette, J., Becker, A.E. and Durrer, D. 1974. A combined morphological and electrophysiological study of the atrioventricular node of the rabbit heart. Circ. Res. **35**: 909–922.
3. Anselm, F., Hook, B., Monahan, K., Frederiks, J., Callans, D., Zardini, M., Epstein, L.M., Zebede, J. and Josephson, M.E. 1996. Heterogeneity of retrograde fast-pathway conduction pattern in patients with atrioventricular nodal reentry tachycardia: observations by simultaneous multisite catheter mapping of Koch's triangle. Circulation **93**: 960–968.
4. Chen, S.A., Chiang, C.E., Tsang, W.P., Hsia, C.P., Wang, D.C., Yeh, H.I., Ting, C.T., Chuen, W.C., Yang, C.J., Cheng, C.C., Wang, S.P., Chiang, B.N. and Chang, M.S. 1993. Selective radiofrequency catheter ablation of fast and slow pathways in 100 patients with atrioventricular nodal reentrant tachycardia. Am. Heart. J. **125**: 1–10.
5. Cox, J.L., Holman, W.L. and Cain, M.E. 1987. Cryosurgical treatment of atrioventricular reentrant tachycardia. Circulation **76**: 1329–1336.
6. de Bakker, J.M.T., Coronel, R., McGuire, M.A., Vermeulen, J.T., Opthof, T., Tasseron, S., van Hemel, N.M. and Defauw, J.A.M. 1994. Slow potentials in atrioventricular junctional area of patients operated on for atrioventricular node tachycardias and in isolated porcine hearts. J. Am. Coll. Cardiol. **23**: 709–715.
7. de Carvalho, A.P. and de Almedia, D.F. 1960. Spread of activity through the atrioventricular node. Circ. Res. **8**: 801–809.
8. Engelstein, E.D., Stein, K.M., Markowitz, S.M. and Lerman, B.B. 1996. Posterior fast atrioven-tricular node pathways: implications for radiofrequency catheter ablation of atrioventricular node reentrant tachycardia. J. Am. Coll. Cardiol. **27**: 1098–1105.
9. Epstein, L.M., Lesh, M.D., Griffin, J.C., Lee, R.J. and Scheinman, M.M. 1995. A direct midseptal approach to slow atrioventricular nodal pathway ablation. PACE **18**: 57–64.
10. Goldberger, J., Brooks, R. and Kadish, A. 1992. Physiology of "atypical" atrioventricular junctional reentrant tachycardia occurring following radiofrequency catheter modification of the atrioventricular node. PACE **15**: 2270–2282.
11. Goy, J.J., Fromer, M., Schlaepfer, J. and Kappenberger, L. 1990. Clinical efficacy of radiofrequency current in the treatment of patients with atrioventricular node reentrant tachycardia. J. Am. Coll. Cardiol. **16**: 418–423.
12. Haissaguerre, M., Gaita, F., Fischer, B., Commenges, D., Montserrat, P., d'Ivernois, C., Lemetayer, P. and Warin, J.F. 1992. Elimination of atrioventricular nodal reentrant tachycardia using discrete slow potentials to guide application of radiofrequency energy. Circulation **85**: 2162–2175.
13. Hintringer, F., Hartikainen, J., Davis, D.W., Heald, S.C., Gill, J.S., Ward, D.E. and Rowland, E. 1995. Prediction of atrioventricular block during radiofrequency ablation of the slow pathway of the atrioventricular node. Circulation **92**: 3490–3496.
14. Hiraoka, A., Karakawa, S., Yamagata, T., Matsuura, H. and Kajiyama, G. 1998. Structural Characteristics of Koch's triangle in patients with atrioventricular node reentrant tachycardia. Hiroshima J. Med. Sci. **47**: 7–15.
15. Inoue, S. and Becker, A.E. 1998. Posterior extensions of the human compact atrioventricular node: a neglected anatomical feature of potential clinical significance. Circulation **97**: 188–193.
16. Jackman, W.M., Beckman, K.J., McClelland, J.H., Wang, X., Friday, K.J., Roman, C.A., Moulton, K.P., Twidale, N., Hazlitt, H.A., Prior, M.I., Oren, J., Overholt, E.D. and Lazzara, R. 1992. Treatment of supraventricular tachycardia due to atrioventricular nodal reentry by radiofrequency catheter ablation of slow-pathway conduction. N. Engl. J. Med. **327**: 313–318.
17. James, T.N. and Sherf, L. 1968. Ultrastructure of the human atrioventricular node. Circulation **37**: 1049–1070.
18. Jazayeri, M.R., Hempe, S.L., Sra, J.S., Dhala, A.A., Blanck, Z., Deshpande, S.S., Avitall, B., Krum, D.P., Gilbert, C.J. and Akhtar, M. 1992. Selective transcatheter ablation of the fast and slow pathways using radiofrequency energy in patients with atrioventricular nodal reentrant tachycardia. Circulation **85**: 1318–1328.
19. Josephson, M.E. 1993. Supraventricular tachycardias, p. 181–274. *In* M.E. Josephson (ed.), Clinical Cardiac Electrophysiology. Lea & Febiger, Philadelphia.
20. Kalbfleisch, S.J., Strickberger, S.A., Williamson, B., Vorperian, V.R., Man, C., Hummel, J.D., Langberg, J.J. and Morady, F. 1994. Randomized comparison of anatomic and electrogram mapping approaches to ablation of the slow pathway of atri-

oventricular node reentrant tachycardia. J. Am. Coll. Cardiol. **23:** 716–723.

21. **Kay, G.N., Epstein, A.E., Dailey, S.M. and Plumb, V.J.** 1992. Selective radiofrequency ablation of the slow pathway for treatment of atrioventricular nodal reentrant tachycardia: evidence for involvement of perinodal myocardium within the reentrant circuit. Circulation **85:** 1675–1688.

22. **McGuire, M.A., Bourke, J.P., Robotin, M.C., Johnson, D.C., Merdrum-Hanna, W., Nunn, G.R., Uther, J.B. and Ross, D.L.** 1993. High resolution mapping of Koch's triangle using sixty electrodes in humans with atrioventricular junctional (AV nodal) reentrant tachycardia. Circulation **88:** 2315–2328.

23. **McGuire, M.A., de Bakker, J.M.T., Vermeulen, J.T., Opthof, T., Becker, A.E. and Janse, M.J.** 1994. Original and significance of double potentials near the atrioventricular node: correlation of extracellular potentials, intracellular potentials, and histology. Circulation **89:** 2351–2360.

24. **McGuire, M.A., Janse, M.J. and Ross, D.L.** 1993. "AV nodal" reentry: part II: "AV nodal, AV junctional or atrionodal" reentry? J. Cardiovasc Electrophysiol. **4:** 573–586.

25. **McGuire, M.A., Johnson, D.C., Robtin, M., Richards, D.A., Uther, J.B. and Ross, D.L.** 1992. Dimensions of the triangle of Koch in humans. Am. J. Cardiol. **70:** 829–830.

26. **Mitrani, R.D., Klein, L.S., Hackett, F.K., Zipes, D.P. and Miles, W.M.** 1993. Radiofrequency ablation for atrioventricular node reentrant tachycardia: comparison between fast (anterior) and slow (posterior) pathway ablation. J. Am. Coll. Cardiol. **21:** 432–441.

27. **Moulton, K., Miller, B., Scott, J. and Woods, W.T.** 1993. Radiofrequency catheter ablation for AV nodal reentry: a technique for rapid transection of the slow AV nodal pathway. PACE **16:** 760–768.

28. **Prichett, L.C., Anderson, R.R., Benditt, D.G., Kasell, J., Harison, L., Wallace, A.G., Sealy, W.C. and Gallagher, J.J.** 1979. Reentry within the atrioventricular node: surgical cure with preservation of atrioventricular conduction. Circulation **60:** 440–446.

29. **Racker, D.K.** 1989. Atrioventricular node and input pathways: a correlated gross anatomical and histological study of the canine atrioventricular junctional region. Anat. Rec. **224:** 336–354.

30. **Ross, D.L., Johnson, D.C., Denniss, A.R.,**

Cooper, M.J., Richards, D.A. and Uther, J.B. 1985. Curative surgery for atrioventricular junctional ("AV nodal") reentrant tachycardia. J. Am. Coll. Cardiol. **6:** 1383–1392.

31. **Tai, C.T., Chen, S.A., Chiang, C.E., Lee, S.H., Chiou, C.W., Ueng, K.C., Wen, Z.C., Chen, Y.Z. and Chang, M.S.** 1996. Multiple anterograde atrioventricular node pathways in patients with atrioventricular node reentrant tachycardia. J. Am. Coll. Cardiol. **28:** 725–731.

32. **Thakur, R.K., Klein, G.J., Yee, R. and Stites, H.W.** 1993. Junctional tachycardia: a useful marker during radiofrequency ablation for atrioventricular node reentrant tachycardia. J. Am. Coll. Cardiol. **22:** 1706–1710.

33. **Truex, R.C. and Smythe, M.Q.** 1967. Reconstruction of the human atrioventricular node. Anat. Rec. **158:** 11–19.

34. **Ueng, K.C., Chen, S.A., Chiang, C.E., Tai, C.T., Lee, S.H., Chiou, C.W., Wen, Z.C., Tseng, C.J., Chen, Y.J., Yu, W.C., Chen, C.Y. and Chang, M.S.** 1996. Dimension and related anatomical distance of Koch's triangle in patients with atrioventricular nodal reentrant tachycardia. J. Cardiovasc. Electrophysiol. **7:** 1017–1023.

35. **Wathen, M.W., Natale, A., Wolfe, K., Tee, R., Newman, D. and Klein, G.** 1992. An anatomically guided approach to atrioventricular node slow pathway ablation. Am. J. Cardiol. **70:** 886–889.

36. **Woods, W.T., Sherf, L. and James, T.N.** 1982. Structure and function of specific regions in the canine atrioventricular node. Am. J. Physiol. **243:** H41–H50.

37. **Wu, D., Yeh, S.J., Wang, C.C., Wen, M.S. and Lin, F.C.** 1993. A simple technique for selective radiofrequency ablation of the slow pathway in atrioventricular node reentrant tachycardia. J. Am. Coll. Cardiol. **21:** 1612–1621.

38. **Wu, D., Yeh, S.J., Wang, C.C., Wen, M.S., Chun, H.J. and Lin, F.C.** 1992. Nature of dual atrioventricular node pathways and the tachycardia circuit as defined by radiofrequency ablation technique. J. Am. Coll. Cardiol. **20:** 884–895.

39. **Yamane, T., Iesaka, Y., Goya, M., Takahashi, A., Fujiwara, H. and Hiraoka, M.** 1999. Optimal target site for slow AV nodal pathway: possibility of predetermined focal mapping approach using anatomic reference in the Koch's triangle. J. Cardiovasc. Electrophysiol. **10:** 529–537.